Corrosion protection performance of cold plasma deposited organosilicon coating: effect of surface pretreatments

Maryem ESBAYOU[1,2], Fouad BENTISS[1,2], Abdelhamid Nyassi[2], Charafeddine JAMA[1,*]

[1]UMET-ISP, CNRS UMR 8207, ENSCL, Université Lille Nord de France, CS 90108, F-59652 Villeneuve d'Ascq Cedex, France
[2]Laboratoire de Catalyse et de Corrosion des Matériaux (LCCM), Faculté des Sciences, Université Chouaib Doukkali, B.P. 20, M-24000 El Jadida, Morocco

Abstract

In order to study the corrosion protection behavior of organosilicon coatings prepared using cold remote nitrogen plasma assisted polymerization of 1,1,3,3-tetramethyldisiloxane (TMDSO), the effect of different surface pre-treatment was tested. The structural properties of the deposited films were analyzed using different methods such as Fourier Transform Infrared Spectroscopy (FTIR), ^{29}Si magic angle spinning NMR (^{29}Si MAS NMR), Scanning Electron Microscopy (SEM), cross-cut, contact angle measurements and profilometery. The corrosion tests were performed by immersing the uncoated and coated carbon steel samples in aerated 3 wt.% NaCl at 30 °C. The protection efficiency against corrosion of the deposited films has been demonstrated by coupling different electrochemical techniques such as open circuit potential (OCP) and electrochemical impedance spectroscopy (EIS). The results clearly demonstrate that the obtained films provide very good barrier against corrosion and show that the protection efficiency depends strongly on pre-treatment conditions.

Keywords: TMDSO; Organosilicon coating, carbon steel, PECVD; EIS.

* Corresponding author. Tel.: +33-320-434-482; fax: +33-320-436-584
E-mail address: charafeddine.jama@ensc-lille.fr (C. JAMA).

Introduction

Plasma enhanced chemical vapor deposition (PECVD) is one of the widely used surface modification plasma process which can produce thin layers of inorganic glassy barrier materials [1]. The biggest advantage of plasma polymerization is that the films can be directly attached to a desired surface while the coatings are growing. In plasma polymerization, the term plasma does not mean a kind of activated species propagating polymeric chains; it means an energy source that initiate polymerization reactions. Compounds with polymerizing structure are required for conventional way of polymerization; however any organic or inorganic compounds can be used in the case of plasma polymerization processes [2-5]. Then, the coatings formed by plasma polymerization are very unique in comparison to classical polymers formed by others processes of polymerization. Plasma polymerization happens owing to the fact that reactive species of the plasma have energy enough to create free radicals which recombination involves the growth of a film. The use of organosilicon monomers was largely developed in order to obtain protective layers which can be used for various applications [2,6,7]. Plasma polymerization of organosilicon coatings leads to films highly cross-linked showing a good resistance to water permeation and hydrophobic appearance[2].

The present work presents a cold plasma polymerization of TMDSO monomer induced by a remote plasma enhanced chemical vapor deposition (denoted RPECVD), located far from the discharge zone, in which the dissociation of the TMDSO monomer is initiated by atomic nitrogen. A number of works have been published using remote nitrogen plasma polymerization of TMDSO for the elaboration of polysiloxane-like coatings (ppTMDSO) for several applications [4,8-11], such as fire retardant protection of polymers [12] or catalytic applications [4,8,13]. The film composition and properties are function of the plasma process parameters and the type of the monomer used [14-17]. This study deals with the corrosion behaviour of carbon steel protected using ppTMDSO films. The effect of surface pretreatment carried out before the deposition of the ppTMDSO film is discussed. Different kinds of surface pretreatments are tested: nitrogen plasma, argon plasma and chemical amorphous phosphatation. Scanning Electron Microscopy (SEM), FT-IR and solid state NMR have been also used to determine the film structure. The corrosion protection properties are evaluated using open circuit potential (OCP) and electrochemical impedance spectroscopy (EIS) measurements in NaCl 3 wt.% solution.

Experimental

Materials

The used monomer was 1,1,3,3-tetramethyldisiloxane (TMDSO) grade 97%, which was supplied from Sigma Aldrich (France), absolute ethanol (grade 99.8% used for washing) and pure water were purchased from VWR (FRANCE). These products were used as received without further purification. The molecular structure of TMDSO is given in Fig. 1.

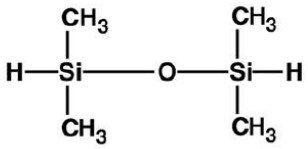

Fig.1. Molecular structure of TMDSO.

The substrates used in this study were carbon steel plates provided by Weber Metaux with the following chemical composition (in wt%) of 0.680% Mn, 0.370% C, 0.230% Si, 0.160% Cu, 0.077% Cr, 0.059% Ni, 0.016% S, 0.011% Ti, 0.009% Co and the remainder is iron (Fe). Samples ($11 \times 9 \times 0.3$ cm^3) were polished using grinding machine with emery paper (SiC 180) for cleaning all of blight, then, were manually polished with other SiC emery papers (240, 400, 1200), rinsed with distilled water, sonicated with absolute ethanol for 10 min and dried before use. After this pretreatment process, surface arithmetic average roughness (R_a) and root mean square roughness (R_q) [18] were determined using a profilometer (Alpha-step IQ, France), and were found to be approximately 0.045 µm and 0.055 µm, respectively.

Plasma polymerization process

The schematic representation of the experimental set-up, presented in Fig. 2, has been previously described in others works [2,4]. A nitrogen plasma discharge was created by a microwave generator (2450± 25 MHz) via a coaxial coupling device in a quartz tube (19 mm inner diameter). Nitrogen gas (grade 99.99%) was introduced by a continuous pumping (primary pump Pfeiffer of nominal flow 344 m^3/h powered by a roots Pfeiffer vacuum), the excited nitrogen species flow from the discharge to the deposition zone (located 1.1 m from the discharge) where the cold remote nitrogen plasma (CRNP) appears as a yellow afterglow. The main reactive species of the CRNP, which is free of charged particles, are atomic nitrogen in the ground electronic state $N(^4S)$ and vibrationally excited nitrogen in the ground electronic state $N_2(X^1\Sigma^+g)_v$ [2]. The nitrogen flow rate was kept constant by means of MKS mass-flow controller (3 slpm). The reactive gases TMDSO monomer mixed with oxygen were introduced in the reaction chamber (height 60 cm and diameter 30 cm) through a coaxial injector Pyrex tube. The distance between the substrate and the injector is 15 cm. The flow rates of dioxygen and TMDSO monomer were 100 sccm and 5 sccm respectively. These deposition parameters were determined thanks to an experimental design taking into account three responses: contact angle, thickness and adhesion. Before applying the protective coating, surface preparation is usually required to clean the substrate, desorb contaminants, reduce the surface roughness, which aims to ensure a good interaction between the coating and the surface. Three different conditions of pretreatment were carried out:

i) Pretreatment using amorphous phosphation with dilute phosphoric acid. The used protocol is given in Table 1 as described previously [19].

Table 1. Amorphous phosphatation pretreatment conditions

Denomination	*Amorphous phosphatation*
Pa	1) Phosphating in H_3PO_4 solution (pH=3) for 10 min at 60°C 2) Rinsing with cold distilled water for 1 min 3) Rinsing with hot distilled water for 1 min (60°C) 4) Drying at 50°C for 15 min.

ii) Pretreatment using cold Radiofrequency Argon plasma (13.56 MHz) generated by a EUROPLASMA CD 1200 apparatus. The detailed protocol is given in previous works [20-22] and the treatment conditions were: treatment duration = 900s, Argon flow rate = 500 sccm, power = 500 W.
iii) Pretreatment using CRNP were: treatment duration = 300s, Nitrogen flow rate = 3 slpm, power = 900 W.

After the pretreatment, the TMDS/O_2 mixture was added during the deposition step in the CRNP zone. TMDSO monomer and dioxygen flow rates were equal to 5 sccm and 100 sccm respectively. Deposition time was fixed to 24 min. The sample-holder was placed in the center of the reaction chamber. Thickness of the coating was measured using a profilometer (Alpha-step IQ, France). The evaluation of the hydrophobicity of the organosilicon deposition was performed through static contact angle measurements at room temperature on a Digidrop goniometer (GBX, France) and was found to be 100 ± 2°, reported as an average of 5 measurements for both methods. The adhesion of these coatings were also evaluated on a metal substrate by cross-cut method and were found a level of 5B.

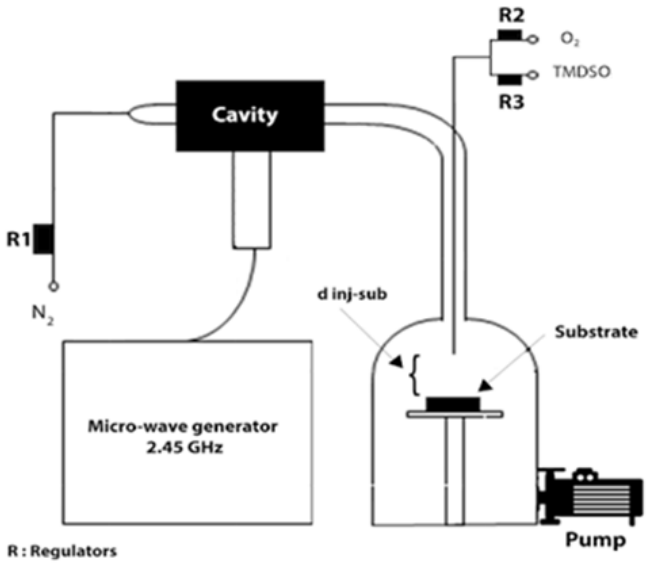

Fig. 2. Schematic representation of the experimental set-up of cold plasma polymerization process.

Characterization methods

Fourier Transforms Infrared spectroscopy (FTIR)

The films were analyzed by a Nicolet 400 impact D FT-IR spectroscopy. Spectra were recorded between 4000 and 400 cm^{-1} (resolution 4 cm^{-1}, 64 scans) in an attenuated total reflectance (ATR) mode. The IR spectra were then plotted and analyzed with the OMNIC software.

Scanning electron microscopy (SEM)

The morphology of the films was studied by scanning electron microscopy (Hitachi S4700) filed emission gun operating with a 5 kV working voltage and a current of 15µA. Specimens for surface morphology were metalized before analysis. The analyzed volume of the specimens was estimated to be approximately (1µm × 1µm × 1µm).

^{29}Si MAS NMR

A mass of ppTMDSO (1.27g) was analyzed with solid state NMR using Bruker Avance – 400 spectrometer at a magnetic field strength of 9.4 T. The ^{29}Si MAS NMR spectra were collected using a 7 mm diameter rotor at 128 scans with a 30° pulse of 2 µs and a relaxation delay of 60 s at a frequency of 79.48 MHz. A software was used for the processing and analysis of obtained NMR spectra.

Electrochemical corrosion test

Electrochemical properties of coated and uncoated steel in a saline (3 wt.% NaCl) solution were characterized at the first by the open circuit potential (OCP) for coated and uncoated samples during a period of two hours, then, subsequently by electrochemical impedance spectroscopy (EIS) using a potentiostat Solartron SI 1287 for impedance measurements and a Solartron 1255B frequency response analyzer. Electrochemical tests were performed in a polymethyl methacrylate (PMMA) cell with a capacity of 1000 ml at 30 ± 1 °C, with a standard three electrodes configuration consisting of the sample as working electrode, a conventional saturated calomel electrode (SCE) as the reference and a Pt electrode as the counter electrode. The working electrode was prepared from a square plate of carbon steel and the area exposed to solution was 7.55 cm^2. ZPlot 2.80 software was used to run the tests and to collect the experimental data. The response of the electrochemical system to ac excitation with a frequency ranging from 10^5 Hz to 10^{-2} Hz and peak to peak amplitude of 10 mV was measured with data density of 10 points per decade. Impedance (Nyquist and Bode plots) data were analyzed with the simulation software Zview 2.80.

Results and discussion

FTIR study

The ppTMDSO (5.45 µm thick films) was analyzed by FTIR spectroscopy in order to get its chemical nature. The FTIR spectra of TMDSO and ppTMDSO are presented in Fig. 3 3. Band assignments were determined according to [4,12,23-26] and are listed in Table 2. Methyl groups, present both in the monomer (TMDSO) and the deposited film, lead to common absorption peaks in both samples: the asymmetric and symmetric $CH_3(\nu(CH_3))$ stretch at 2960 and 2910 cm^{-1} respectively, the $CH_3(\delta(CH_3))$ asymmetric and symmetric bending in Si-CH_3 at 1410 and 1259 cm^{-1} and a group of absorption bands between 900 and 700 cm^{-1} are assigned to the methyl rocking mode and the SiC stretching mode in $Si(CH_3)_x$.

The FTIR of ppTMDSO film (Fig. 3B) is marked by:

i) The decrease of the strong band at 2220 cm^{-1}, characteristic of the Si-H stretching band, which gives evidence of the H ablation [4].
ii) At around 1015 cm^{-1}, the enhancement and strong broadening of this peak, characteristic of the asymmetrical elongation of the Si-O-Si band in a polymeric siloxane conformation.
iii) The appearance of a broad band located at around 3315 cm^{-1} corresponding to a silanol band (Si-OH).

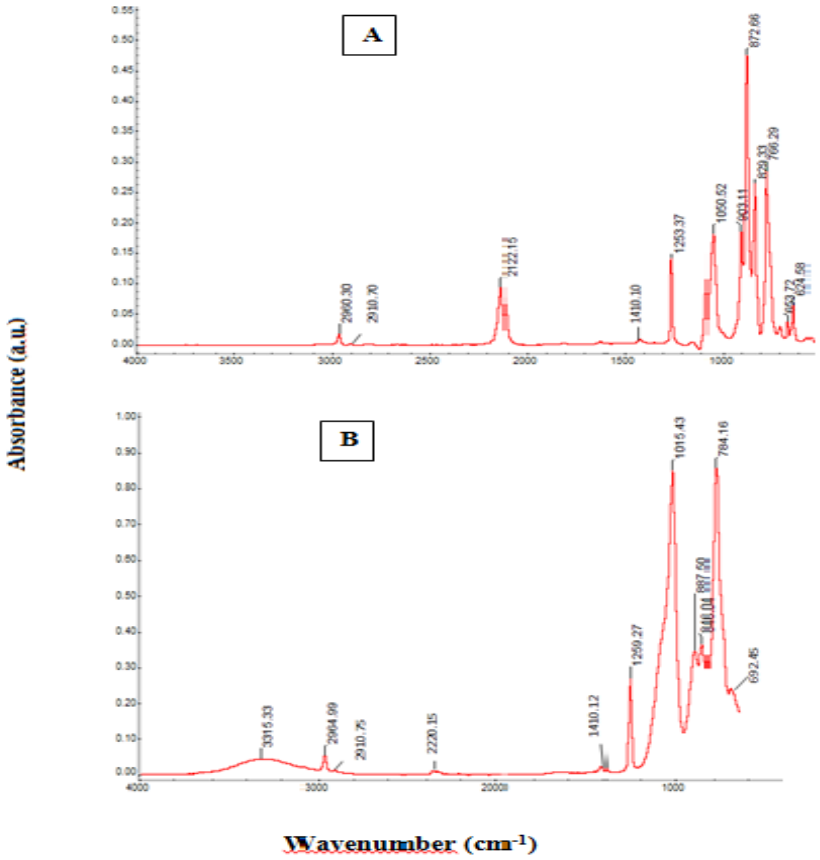

Fig. 3. FTIR spectra of the monomer (A); of ppTMDSO film (thickness 5.45µm) as deposited treated for 5 min by N_2 (B).

Table 2. Bands assignments

Peak position (cm^{-1})	Assignments
3315	ν(OH), Si-OH
2964	$\nu(CH_3)_{as}$
2910	$\nu(CH_3)_s$
2220	ν(Si-H)
1410	$\delta(CH_3)_{as}$, $Si-(CH_3)_x$
1259	$\delta(CH_3)_s$, $Si-(CH_3)_2$
1015	$\nu(Si-O-Si)_{as}$
887	$\delta(CH_3)$, ν(Si-C), $Si-(CH_3)_2$
846	$\delta(CH_3)$, ν(Si-C), $Si-(CH_3)_2$
784	ν(Si-C), $Si-(CH_3)_2$
692	ν(Si-C)

Solid and liquid state NMR study

Solid state ^{29}Si NMR spectrum of ppTMDSO (Fig. 4) shows a complex structure significantly different from that of TMDSO, which is known to give rise to a single resonance line at approximately -5 ppm (M^H) [22,27]. ^{29}Si MAS NMR spectra show four main groups of resonance lines, which correspond to four siloxane moieties that are: M, D, T and Q, which relates to the number of O atoms bonded to Si atom. Fig. 4 shows that there are 8 clearly distinguishable peaks positioned at isotopic chemical shifts, δ (^{29}Si) of different intensities detailed in Table 3. This can be explained by the fact that there is no limitation on the bonds that can be formed in contrast to traditional polymerization, and, hence, Si atoms are observed in a wide range of bonding environments. One can note that the presence at -11.5 ppm reflects the chemical structure of the monomer TMDSO indicating that the polymerization is incomplete. The presence of the Si-H bond is also consistent with the result obtained by FTIR spectroscopy. The most oxidized configuration, Q, seems to be in a weak proportion compared to D and T configurations.

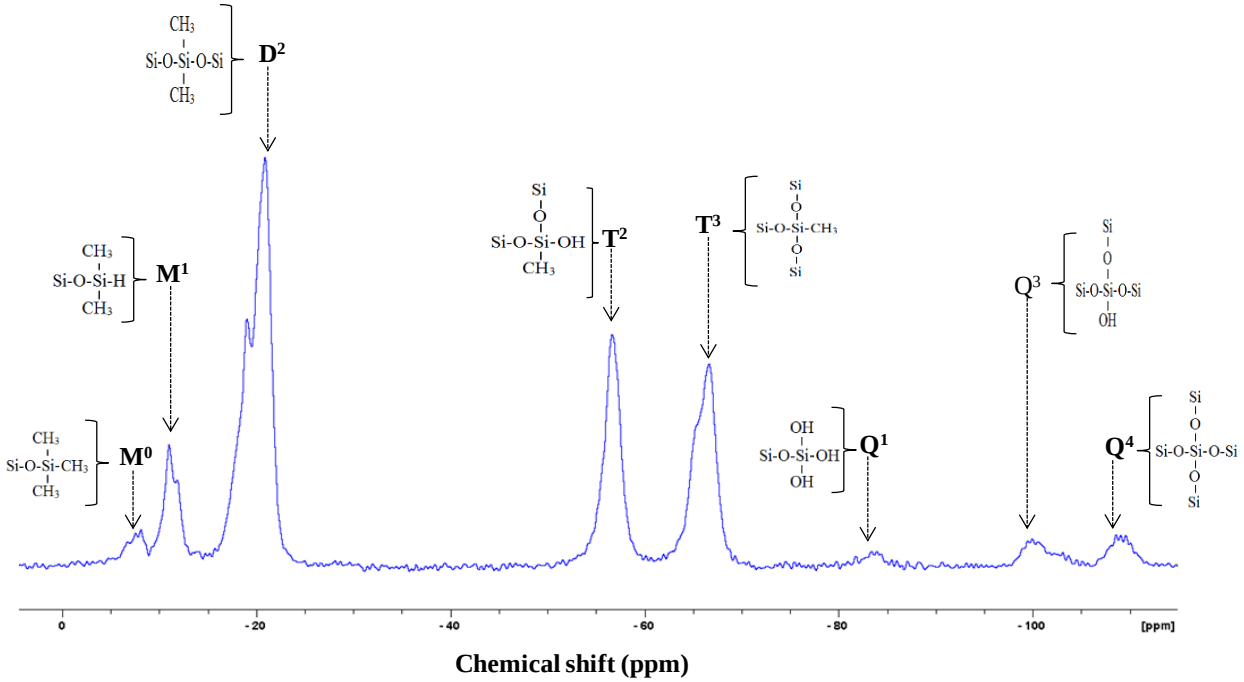

Fig. 4. ^{29}Si NMR spectrum obtained from the organosilicon coating using TMDSO as precursor.

Table 3. Solid state ^{29}Si MAS NMR peaks with their chemical shifts, integral intensity and assigned structures.

Assignment	M^0	M^1	D^2	T^2	T^3	Q^1	Q^3	Q^4
δ (^{29}Si) (ppm)	-8.14	-11.5	-19.06	-56.69	-66.68	-83.90	-100.70	-109.08
Integral intensity (%)	1.35	8.11	49.32	19.24	21.59	0.87	0.55	0.72

Scanning electron microscopy (SEM)

The Fig. 5 presents SEM images of uncoated and ppTMDSO coated steel. Its shows the microstructure obtained using different pretreatments. The coating pretreated using amorphous phosphatation presents a heterogeneous structure with granular particles. Argon plasma pretreatment presents a morphology in which one can see the presence of some particles while nitrogen plasma pretreatment leads to more homogeneous coating. These results indicate that the morphology strongly depends on the pretreatment used.

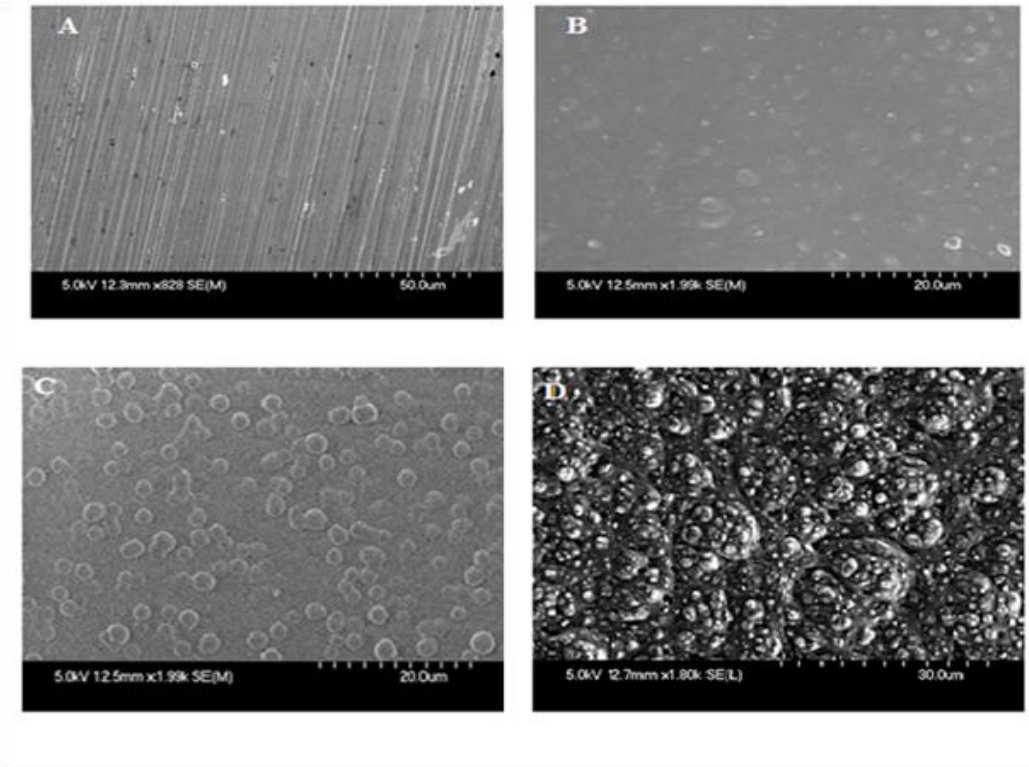

Fig. 5. SEM images of uncoated steel (A) and ppTMDSO coated steel using different pretreatment: nitrogen pretreatment (5.45 µm, 5B) (B); Argon pretreatment (4.28µm, 5B) (C) and phosphate pretreatment (2.75, 2B) (D).

Electrochemical measurement

The variation of OCP as a function of immersion time for the uncoated and coated samples in 3 wt.% NaCl at 30°C is presented in Fig. 6. It can be seen that for the organosilicon coating pretreated with nitrogen plasma, OCP seems to be stable after few minutes of immersion and nearly at (+0.49 V/SCE). However, it stabilizes for the other pretreatments: argon plasma and amorphous phosphatation at around -0.34 and -0.45 V/SCE) respectively. This result gives evidence of good isolation properties of organosilicon coatings when it is pretreated with nitrogen plasma.

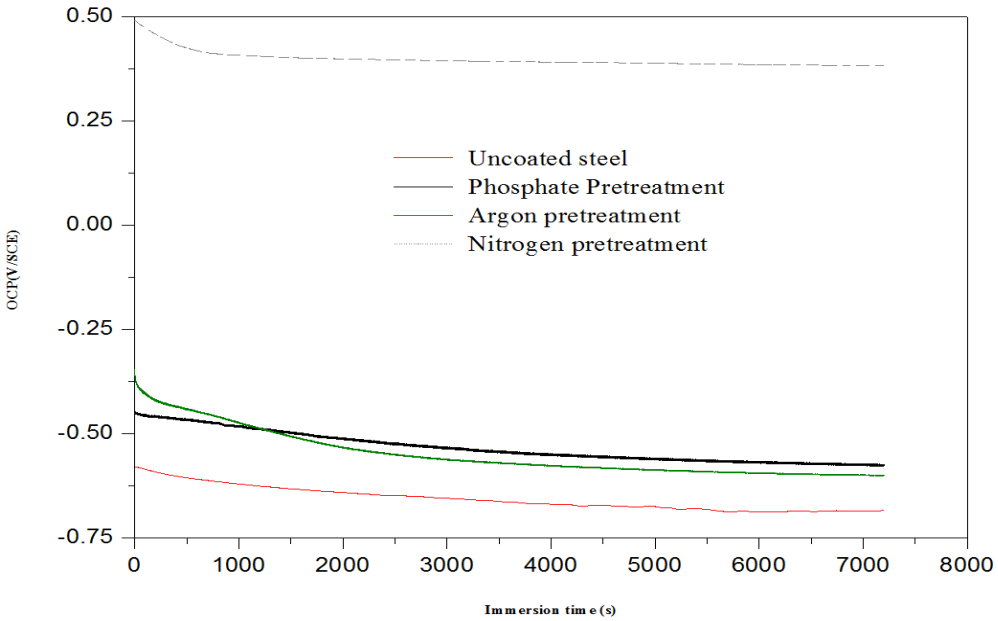

Fig. 6.Open Circuit Potential evolutions as function of immersion time for uncoated and coated samples using different pretreatment in 3 wt.% NaCl solution at 30°C.

The corrosion behavior was also investigated by EIS after 2 h and 336 h of immersion in 3 wt.% NaCl solution at 30°C. Fig. 7 shows the Bode modulus and phase diagrams obtained for uncoated and steel coated using different pre-treatment after 2h of immersion. One can see in phase plots (Fig. 7B), two time-constant for coated samples and only one time-constant at low frequency for uncoated steel are determined. The time constant at high frequency is attributed to the diffusion of electrolytes through the pores of the protective coating. The time constant at low frequency is associated to charge transfer at the interface electrolyte/surface. From modulus diagrams (Fig. 7A), global impedance modulus (|Z| at 0.01Hz) values are determined: 9.43×10^{2}; 2.43×10^{6}, 1.32×10^{5}, 9.14×10^{3} Ω cm^{2} for uncoated and coated steel using nitrogen plasma, argon plasma and amorphous phosphatation pretreatments respectively. The higher values, in comparison to uncoated samples, give evidence of the barrier effect of the coating using nitrogen and argon plasma pretreatments and that this effect is also strongly affected by the nature of the pretreatment. Fig. 8 shows the Bode modulus and Phase diagrams after 336 h of immersion. From Fig. 8A the global modulus (|Z| at 0.01Hz) determined are 7.86×10^{2}; 3.58×10^{5}, 1.06×10^{4}, 7.38×10^{2} Ω cm^{2} for uncoated and coated steel using nitrogen plasma, argon plasma and amorphous phosphatation pretreatments. Modulus values indicate that organosilicon coating pretreated using nitrogen plasma is the most stable as a function of immersion time and shows the best corrosion resistance performance. However, Fig. 8B shows that for amorphous phosphatation pretreatment only one time constant at low frequency is remaining, indicating a total disappearance of the barrier effect of the coating.

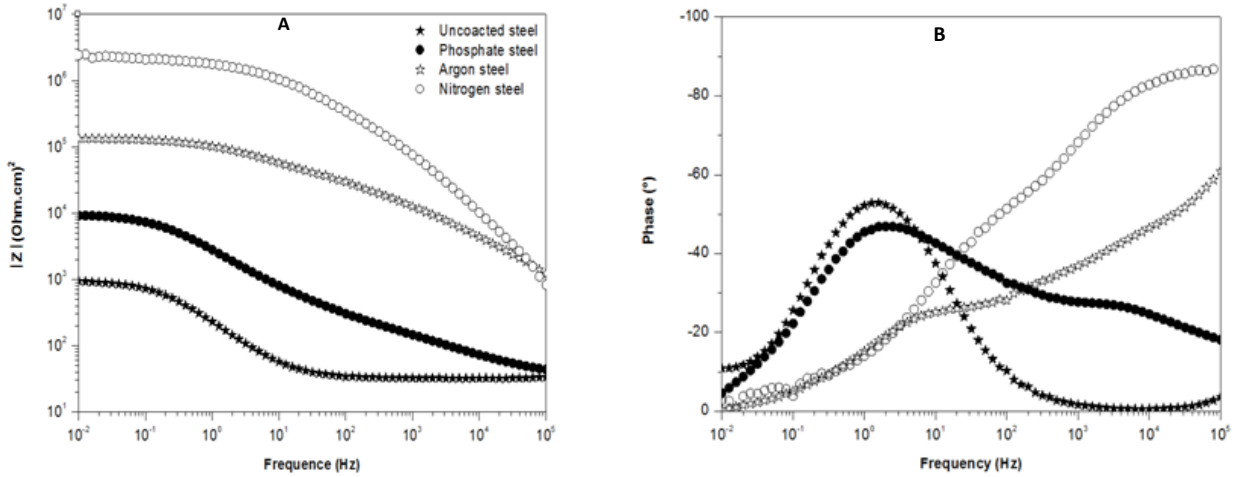

Fig. 7. Bode modulus (A) and phase (B) plots of uncoated and coated samples with different pretreatment in 3 wt.% NaCl solution at 30°C after 2 h of immersion.

The impedance diagrams as function of immersion time for organosilicon coated samples using nitrogen plasma pretreatment are shown in Fig. 9. Global impedance modulus (|Z| at 0.01 Hz) values are determined from Fig. 9A: 2.43×10^6, 1.68×10^6, 3.58×10^5, 9.87×10^4 Ω cm^2 at 2 h, 48 h, 336 h and 576 h, respectively. This means that the global modulus decreases as function of immersion time but remains higher than that of the uncoated steel giving evidence of the persistence of the barrier effect even after 576h of immersion as shown from phase plot in Fig. 9B. This behavior can be attributed to the higher resistance of coating/steel interface due to better adherence and to a denser structure with lower porosity of the organosilicon coating using nitrogen plasma pretreatment.

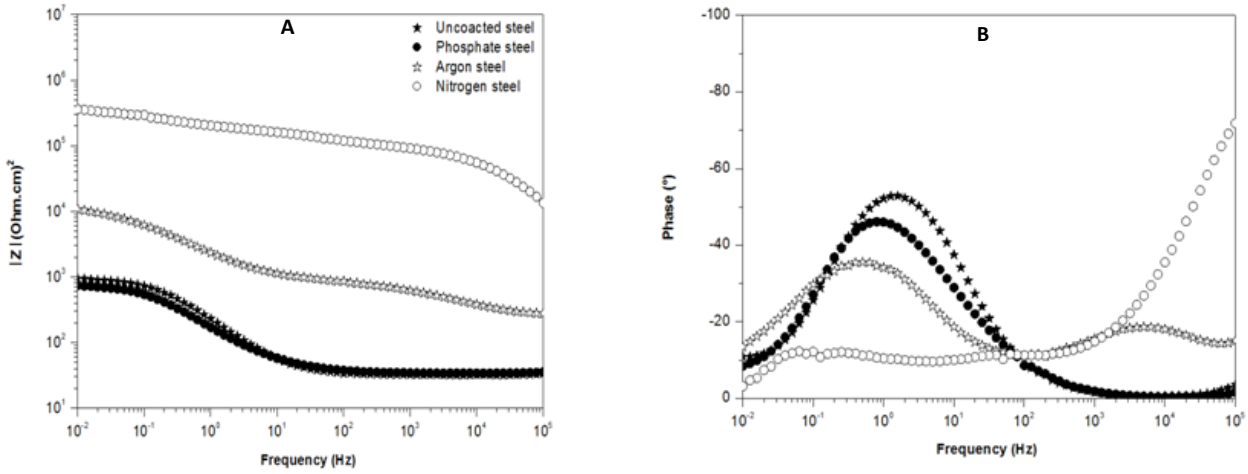

Fig. 8. Bode modulus (A) and phase (B) plots of uncoated and coated samples with different pretreatment in 3 wt.% NaCl solution at 30°C after 336 h of immersion.

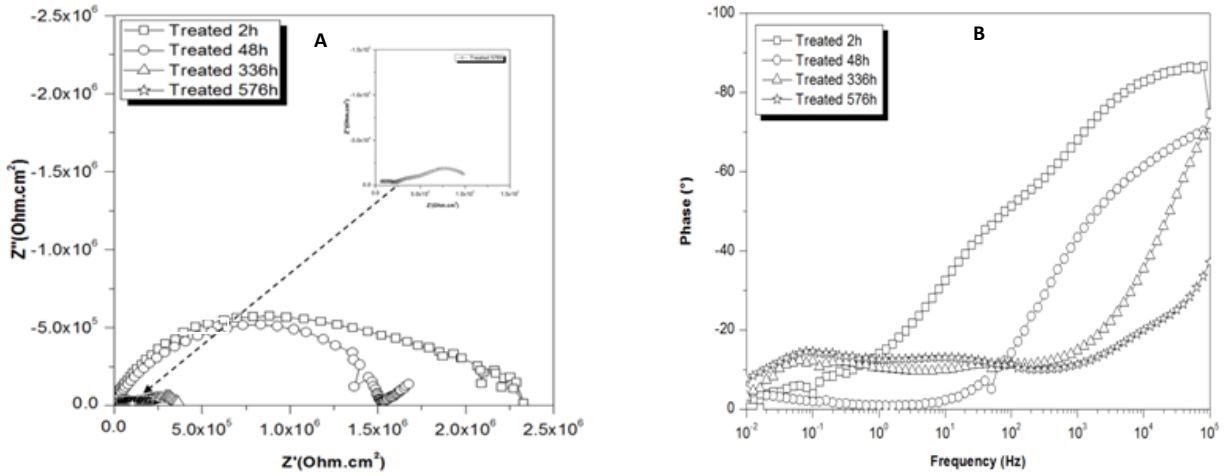

Fig. 9. Nyquist diagrams (A) and phase plots (B) for ppTMDSO using nitrogen pretreatment after 2 h, 48 h, 336 h and 576 h of immersion in 3 wt.% NaCl solution at 30°C.

Conclusions

In this study, the structural properties of the ppTMDSO are investigated using FTIR and solid state ^{29}Si MAS NMR. The effect of different kinds of surface pretreatments are presented: nitrogen plasma, argon plasma and amorphous phosphatation surface carried out before the deposition of ppTMDSO film. The results obtained by SEM show that less porous surface morphology is obtained for coatings with nitrogen plasma pretreatment. EIS results show that the anticorrosion performance is strongly affect by the pretreatment nature and increases in the following order: phosphate pretreatment > argon pretreatment > nitrogen pretreatment. Moreover, using nitrogen pretreatment the global modulus, determined using EIS, decreases as function of immersion time but remains higher indicating the persistence of the barrier effect even after 576h of immersion. This behavior is explained by a better adherence and to dense structure with lower porosity of the organosilicon coating.

Acknowledgments

The authors gratefully acknowledge Campus France and the Moroccan Ministry of Higher Education, Research and Training **(**MESRSFC) for their financial support under the program of Partenariat Hubert Curien PHC Toubkal/15/10 –32471TE.

References

1. H. Gallou, PhD Thesis, Amélioration du comportement au feu du polyamide 6.6 par traitement de surface et en masse, Université Lille Nord de France (2010).
2. N. Ghali, C. Vivien, B. Mutel and A. Rives, Surf. Coat. Technol, **259** (2014) 516.
3. N. Inagaki, Technomic Publishing Company, Lancaster, Pennsylvania, (1996).
4. A. Essakhi B. Mutel, P. Supiot, A. Löfberg, S. Paul, V.L. Courtois, V. Meille, I. Pitault and E. Bordes-Richard, Polym. Eng. Sci., **51**(2011) 947.
5. H.Yasuda and C.E. Lamaze, J. Appl. Polym. Sci. **17** (1973) 1531.

6. A. Delimi, Y. Coffinier, B. Talhi, R. Boukherroub and S. Szunerits, Electrochim. Acta, **55** (2010) 8927.
7. G. Czeremuszkin, M. Latreche, M.R. Wertheimer and A.S. Da Silva sobrinho, Plasma Polym., **6** (2001) 107.
8. L. Guillou, P.Supiot, and V. Le courtois, Surf. Coat. Technol., **202** (2008) 4233.
9. L. Guillou, D. Balloy, P. Supiot, and V. Le courtois, Appl. Catal., A, **324** (2007) 42.
10. L. Guillou, V. Le Courtois, and P. Supiot, Mater. Technol., **93** (2005) 335
11. F. Callebert, P. Supiot, K. Asfardjani, O. Dessaux, P. Goudmand, P. Dhamelincourt, J. Laureyns, J. Appl. Polym. Sci. **52** (1994) 1606. .
12. A. Quédé, B. Mutel, P. Supiot, C. Jama, O. Dessaux, and R. Delobel, Surf. Coat. Technol., **181** (2004) 270.
13. A. Essakhi, A. Löfberg, S. Paul, B. Mutel, P. Supiot, V. Le Courtois, P. Rodriguez, V. Meille and E. Bordes-Richard, Microporous Mesoporous Mater., **140** (1985) 88.
15. T.J. Lin, B.H. Chun, H.K. Yasuda, D.J. Yasuda, D.J. Yang and J.A. Antonelli, J. Adhes. Sci. Technol., **5** (1991) 893.
16. O. Auciello and D.L. Flamm (eds.), Plasma diagnostics, Vol. 1, Discharge Parameters and Chemistry, Vol. 2, Surface Analysis and Interactions, Academic press, San diego, CA, (1989).
17. R. D'Agostino (ed.), Plasma Deposition Treatment and Etching of Polymers, Academic Press, Boston, (1990).
18. E. Degarmo, P. Black, J. Kohser and A. Ronald, Materials and Processes in Manufacturing (9th ed.), Wiley, (2003) 223.
19. A. Mayot, PhD Thesis, Formation à température ambiante, caractérisation et application à la protection anticorrosion de revêtements adhérents de silice amorphe, Université Lille Nord de France (1990).
20. F.Z. Bouanis, F. Bentiss, M. Traisnel and C. Jama, Electrochim. Acta, **54** (2009) 2378.
21. F.Z. Bouanis, F. Bentiss, M. Traisnel and C. Jama, Corros. Sci., **52** (2010) 3190.
22. F.Z. Bouanis, F. Bentiss, S. Bellayer, J.B. Vogt and C. Jama, Mater. Chem. Phys., **127** (2011) 334.
23. C.J. Hall , T. Ponnusamy, P.J. Murphy, M. Lindberg, O.N. Antzutkin, and H.J.Griesser, ACS Appl. Mater. Interfaces, **6** (2014) 62.
24. W.P. Yang, D. Costa and P. Marcus, J. Electrochem. Soc., **141** (10) (1994) 2676.
25. D.R. Anderson, in: A.L. Smith (Ed.). Infrared, Raman and Ultra violet Spectroscopy: Analysis of silicones, Wiley, London, (1974) 247.
26. A. Grill and D.A. Neumayer, J. Appl. Phys., **94** (2003) 6707.
27. H.C. Marsmann and F. Uhlig, Silicon-29 NMR Data of $C_4H_{14}OSi_2$ Eds.; Springer-Verlag: Berlin, Heidelberg, **35** (2008) 315.